© 2019. Published by The Company of Biologists Ltd | Journal of Experimental Biology (2019) 222, jeb213306. doi:10.1242/jeb.213306

RESEARCH ARTICLE

Diffusive structural colour in *Hoplia argentea*

Cédric Kilchoer[1], Primož Pirih[2], Ullrich Steiner[1] and Bodo D. Wilts[1,*]

ABSTRACT

Nature's nanostructures can bring about vivid and iridescent colours seen in many insects, notably in beetles and butterflies. While the intense structural colours can be advantageous for display purposes, they may also be appealing to predators and therefore constitute an evolutionary disadvantage. Animals often employ absorption and scattering in order to reduce the directionality of the reflected light and thereby enhance their camouflage. Here, we investigated the monkey beetle *Hoplia argentea* using microspectrophotometry, electron microscopy, fluorimetry and optical modelling. We show that the dull green dorsal colour comes from the nanostructured scales on the elytra. The nanostructure consists of a multi-layered photonic structure covered by a filamentous layer. The filamentous layer acts as a spatial diffuser of the specular reflection from the multilayer and suppresses the iridescence. This combination leads to a colour-stable and angle-independent green reflection that probably enhances the camouflage of the beetles in their natural habitat.

KEY WORDS: Iridescence, Insect colours, Pigment filter, Light scattering, Camouflage

INTRODUCTION

Coloration in insects accomplishes a range of different functions, e.g. camouflage or signalling to mates and predators (Berthier, 2007; Doucet and Meadows, 2009; Bradbury and Vehrencamp, 2011; Hubbs, 1942). Pigmentary colour in insects is usually due to organic dyes in the sub-epidermal tissue, the integument and the cuticle. Incident light that is not selectively absorbed by the pigments is isotropically scattered, resulting in dull, angle-independent colour. In contrast, some insects have structural colour that arises from the interaction of incident light with nanostructures in their scales (Srinivasarao, 1999). Periodic nanostructures produce vivid colours (Biró and Vigneron, 2011), which are strongly reflective, iridescent and specular (Doucet and Meadows, 2009). Structural coloration can be observed on butterfly wing scales, and on the cuticle and scales of beetles (Seago et al., 2009; Stavenga et al., 2011a).

Colour is not only used for signalling. When it comes to camouflage, insects mimic the coloration of their environment to remain unnoticed to the eyes of potential predators (Stevens and Merilaita, 2011). Camouflage can be achieved by spectrally adapting to the background (Schaefer and Stobbe, 2006), by transparency (Johnsen, 2001; Siddique et al., 2015; Yoshida et al., 1996) or by broadband reflectivity (Holt et al., 2011; Jordan et al., 2012; Vukusic et al., 2009; Wilts et al., 2013b). The main habitats of most insects – plants, soil and rocks – are generally diffusely reflecting and have reflectance spectra with broad peaks. The strong reflectivity and the colour change of iridescent structures may therefore be disadvantageous for efficient camouflage with these backgrounds. Many beetles and butterflies have evolved methods that suppress iridescence from structural colour by orientational averaging or spectral filtering (Wilts et al., 2012a,b).

A striking example of vivid beetle coloration is demonstrated by the well-investigated males of the monkey beetle species *Hoplia coerulea* (Coleoptera: Scarabaeidae: Hopliini) that possess a multilayered, porous nanostructure which produces a specular reflection with a reflectance peak of 0.6 at blue wavelengths with respect to a mirror (Mouchet et al., 2017; Vigneron et al., 2005). This striking colour is thought to be used to attract females (Rassart et al., 2009). In recent years, *H. coerulea* has received considerable attention because of its water vapour-sensitive optical properties (Mouchet et al., 2016a,b). Many *Hoplia* species exist with few or no scales and a dull brown appearance due to the colour of the cuticle. Here, we investigated the coloration of the elytral scales of *Hoplia argentea* (deprecated synonym *Hoplia farinosa*), a beetle commonly observed across Europe, which has an elytra covered by scales and is a muted green rather than brown. In Alpine regions, such as northern Slovenia and Switzerland, the abundance of *H. argentea* often reaches high levels in the period May–July. The adults inhabit wet places with lush vegetation and may be observed feeding and mating on plants with large inflorescences, e.g. elderberry, umbellifers and plants from the rose family. The females lay their eggs near to the ground, and the larvae feed in the ground on rootlets (Brelih et al., 2010).

In contrast to the strongly sexually dimorphic *H. coerulea*, for which the elytra of males are shiny blue, both sexes of *H. argentea* are dull green and less conspicuous against the vegetation background. This difference was pointed out by Gentil in 1943 in the first attempt to compare the scale ultrastructure of the two species (Gentil, 1943). The origin of the structural coloration was not fully characterized at the time. Here, we show that the coloration of *H. argentea*'s dorsal side results from combining a porous chitin/air multilayer reflector with absorptive filtering and scattering by a brush-like, diffusive layer on the upper (adwing) side of the scales. We discuss the possible function of shedding the scales, which brings about the hue change from green to brown. This change might be an adaptive camouflage mechanism for females that lay the eggs on the ground.

MATERIALS AND METHODS

Study species

Specimens of *Hoplia argentea* (Poda 1761) were captured around Évolène (Switzerland, *N*=2) and around Jezersko and Ilirska Bistrica (both Slovenia, *N*=5) in June and July 2019. Samples were stored in dry (relative humidity <25%) and dark conditions before measurements, which were performed in lab conditions.

[1]Adolphe Merkle Institute, University of Fribourg, Chemin des Verdiers 4, 1700 Fribourg, Switzerland. [2]Department of Biology, Biotechnical Faculty, University of Ljubljana, Vecna pot 111, 1000 Ljubljana, Slovenia.

*Author for correspondence (bodo.wilts@unifr.ch)

C.K., 0000-0001-7453-4142; P.P., 0000-0003-1710-444X; U.S., 0000-0001-5936-339X; B.D.W., 0000-0002-2727-7128

Received 28 August 2019; Accepted 19 November 2019

Journal of Experimental Biology (2019) 222, jeb213306. doi:10.1242/jeb.213306

Optical characterization

Spectral characterization was performed using a xenon light source (SLS401, Thorlabs GmbH, Dachau, Germany) and an Axio Scope.A1 microscope (Zeiss AG, Oberkochen, Germany). The light reflected from the sample was collected using an optical fibre (QP230-2-XSR, 230 µm core) with a measurement spot size of approximately 10 µm, and a protected silver mirror (Thorlabs PF10-03-P01) was used as a reference. The spectra were recorded by a spectrometer (Maya2000 Pro, Ocean Optics, Dunedin, FL, USA). Optical micrographs were captured with a CCD camera (GS3-U3-28S5C-C, Point Grey/FLIR Integrated Imaging Solutions Inc., Richmond, BC, Canada). *k*-space imaging, i.e. a measurement of the far-field reflection, was performed by placing a Bertrand lens (Zeiss 453671) in the imaging pathway, using a high numerical aperture air objective (Zeiss Epiplan Neofluar 50×, NA 0.95).

Fluorescence characterization

Fluorescence images were acquired using a DP72 Colour CCD Camera mounted on a BX51 microscope (all Olympus Corporation, Tokyo, Japan). The excitation/filtering wavelengths for the blue, green and red channels were 330–380 nm/420 nm, 450–480 nm/515 nm and 510–550 nm/590 nm, respectively. Samples were illuminated using a mercury lamp (X-Cite 120Q, Excelitas Technologies Corp., Waltham, MA, USA).

Spectrofluorimetry experiments were performed on parts of the elytra, using a Fluorolog system (Horiba Scientific, Kyoto, Japan). The measurements were performed with a 4 nm bandpass slit for the excitation and a 3 nm bandpass slit for the emission, with 0.1 s integration time. The incident light formed a 30 deg angle with the sample normal. The emitted light was detected at a 60 deg normal angle.

Scanning electron microscopy (SEM)

A wing piece was cut from the beetle and glued onto a standard SEM stub. The sample was imaged using a Scios 2 dual-beam field-emission electron microscope (FEI, Eindhoven, The Netherlands). To prevent charging effects, a 5 nm gold layer was sputtered onto the sample using a 208 HR sputter coater (Cressington Scientific Instruments, Watford, UK).

Optical modelling

The optical simulation was carried out using the transfer-matrix method (Yeh, 2005). The simulated system had six bilayers consisting of a 110±30 nm porous chitin layer and a 95±30 nm solid chitin layer, as estimated from morphological data (means±s.d.). To mimic natural variation, the thickness of each layer in the simulation was taken from this interval. The refractive index used for porous and solid chitin layers was assumed to be 1.10 and 1.55, respectively. The refractive index of the porous layer is slightly above the refractive index of air, n=1.00, in order to account for the filling factor of chitin in the porous layers. In order to account for the layer thickness variation, the reflectance spectrum simulation was repeated 100 times and averaged.

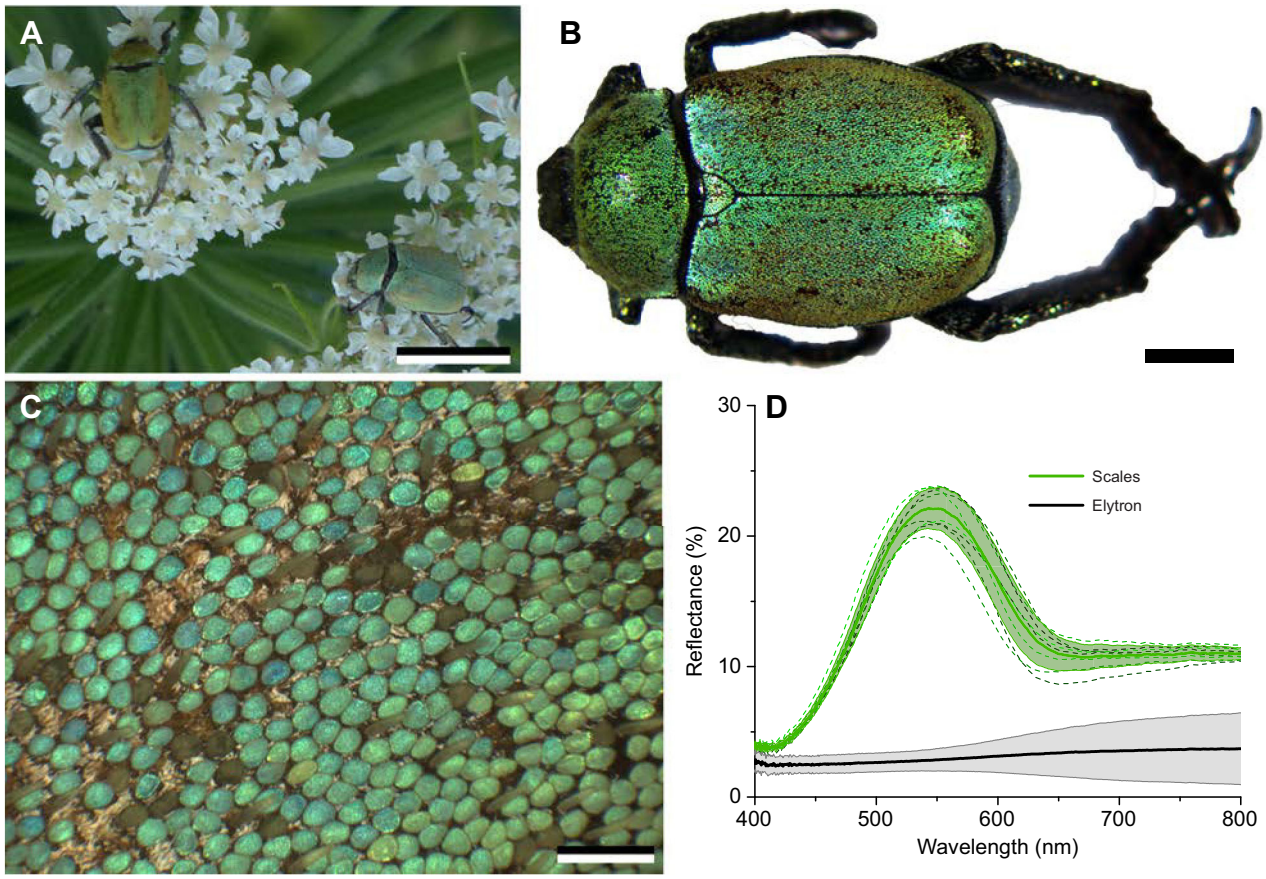

Fig. 1. *Hoplia argentea*. (A) Specimens in their natural habitat. (B) Close-up photograph of a specimen with black–brown cuticle and many scales. (C) Optical micrograph of the beetle elytron. (D) Reflection of the beetle scales (green) and elytron (black). The dashed lines show reflectance spectra from individual cover scales. Solid lines and bands are the means±s.d. of the reflectance spectrum (N=10 scales, N=5 elytron). Scale bars: (A) 10 mm, (B) 2 mm, (C) 200 µm.

Journal of Experimental Biology (2019) 222, jeb213306. doi:10.1242/jeb.213306

RESULTS

Optical appearance and anatomy

Hoplia argentea beetles have a typical body length of around 1 cm (Fig. 1A), with an overall dull green colour on the dorsal side. A closer look of the elytron revealed that a red–brown to black–brown cuticle is covered by green-coloured scales (Fig. 1B). The scales typically have a rounded shape with a diameter of 50±10 µm and lie on the elytron in a single layer (Fig. 1C). The reflection of individual scales and the elytron was spectrally characterized using a custom-built microspectrophotometer. The black–brown elytron has a spectrally flat reflectance below ∼5% at visible wavelengths, indicative of the presence of a broadband-absorbing pigment, probably melanin. In contrast, the green scales exhibit a pronounced reflection peak at ∼540 nm with a full-width at half-maximum of ∼100 nm (Fig. 1D). The dull green coloration of the beetle arises mostly from reflection from the scales. Some animals lose their scales through wear (probably caused by frequent mounting during mating attempts), resulting in a change of the overall hue from dull green to brown (Fig. S3). The iridescent colour of the ventral side of the animals seems to be more consistent among specimens and is due to blue–green, specularly reflecting scales (Fig. S4).

Scale anatomy: pigments and multilayers

To understand the basis of the colour, we investigated the scale anatomy and the presence of pigments. First, a refractive index-matching experiment was conducted to establish the presence of absorbing pigments within the scales (Stavenga et al., 2013). The transmission spectrum of a single scale was recorded in air and immersed in a refractive index fluid of n=1.55 (Fig. S1). The transmittance drastically increased at long wavelengths as interfacial scattering was removed by the index-matching fluid, while the presence of a UV-absorbing pigment with increasing absorbance towards shorter wavelengths (<400 nm) became apparent.

The UV-absorbing pigment is fluorescent (Fig. S2). This allowed imaging of the wing scales (Fig. 2A) using fluorescence microscopy (Fig. 2B) to determine the pigment distribution throughout the scale. The scale in cross-section has a two-tiered structure. The upper, abwing layer contains short filaments. The lower, adwing layer appears solid. The fluorophore can be detected in both tiers, but is predominantly present in the lower layer.

To better resolve the scale ultrastructure, SEM was employed. The top view of a single scale shows a brush-like structure with hundreds of small filaments with a diameter of 480±50 nm and a length of ∼5 µm (Fig. 2C) that are also visible in the fluorescence micrograph of Fig. 2D. The filaments have a rather disorderly arrangement on the scale and do not show a common orientation. The density is estimated to be 65±7 filaments per 10×10 µm^2.

To visualize the optical structure below the filamentous brush, a single scale was sectioned with a focused-ion beam. The scale cross-section in Fig. 2E shows that the ultrastructure is composed of two distinct parts. A filamentous top layer covers a photonic structure consisting of alternating layers of solid and macroporous chitin with a thicknesses of 95±30 and 110±30 nm, respectively. The structure of the photonic multilayer appears to be similar to that observed in the related *H. coerulea* (Mouchet et al., 2016a; Rassart et al., 2009; Vigneron et al., 2005).

Spectral averaging and camouflage

To understand the influence of the scale anatomy on the optical properties, the spatial reflection patterns from single scales were spectrally characterized using a microspectrophotometer (Fig. 3). We illuminated the scale from the abwing side (filaments first) and adwing side (multilayer first) (Fig. 3G). The angular distribution of the reflected and scattered light was characterized in the far-field, using a Bertrand lens. Under narrow-aperture illumination, the specularity of reflected light was investigated. When illuminated

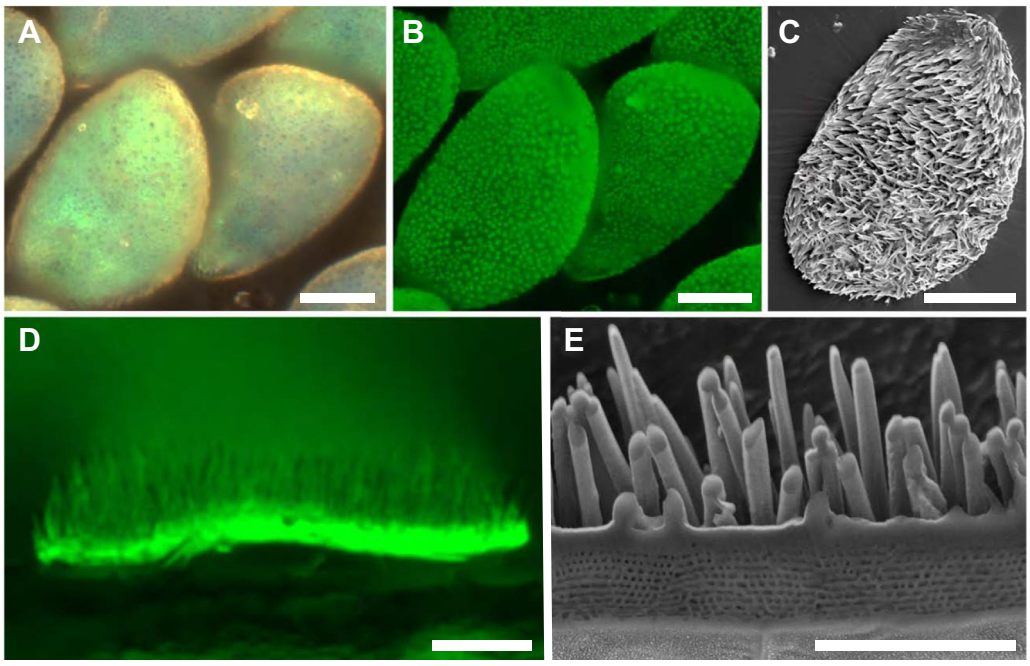

Fig. 2. Scale ultrastructure and fluorescence. (A) Epi-illumination micrograph of the beetle's elytra scales. (B) Fluorescence micrograph of the same scales. (C) Top-view scanning electron micrograph of a single scale. The scale is covered by brush-like filaments. (D) Fluorescence micrograph showing a cross-sectional view of the scale. The source of fluorescence is mostly located in the scale base. (E) Focused ion beam-scanning electron microscope imaging of a scale cross-section. The scale ultrastructure is composed of a porous multilayer photonic crystal below the filament layer on the abwing side. The excitation/filtering wavelengths for the green fluorescence microscopy (B,D) are 450–480 nm/515 nm (see also Fig. S2). Scale bars: (A–C) 20 µm, (D,E) 5 µm.

Journal of Experimental Biology (2019) 222, jeb213306. doi:10.1242/jeb.213306

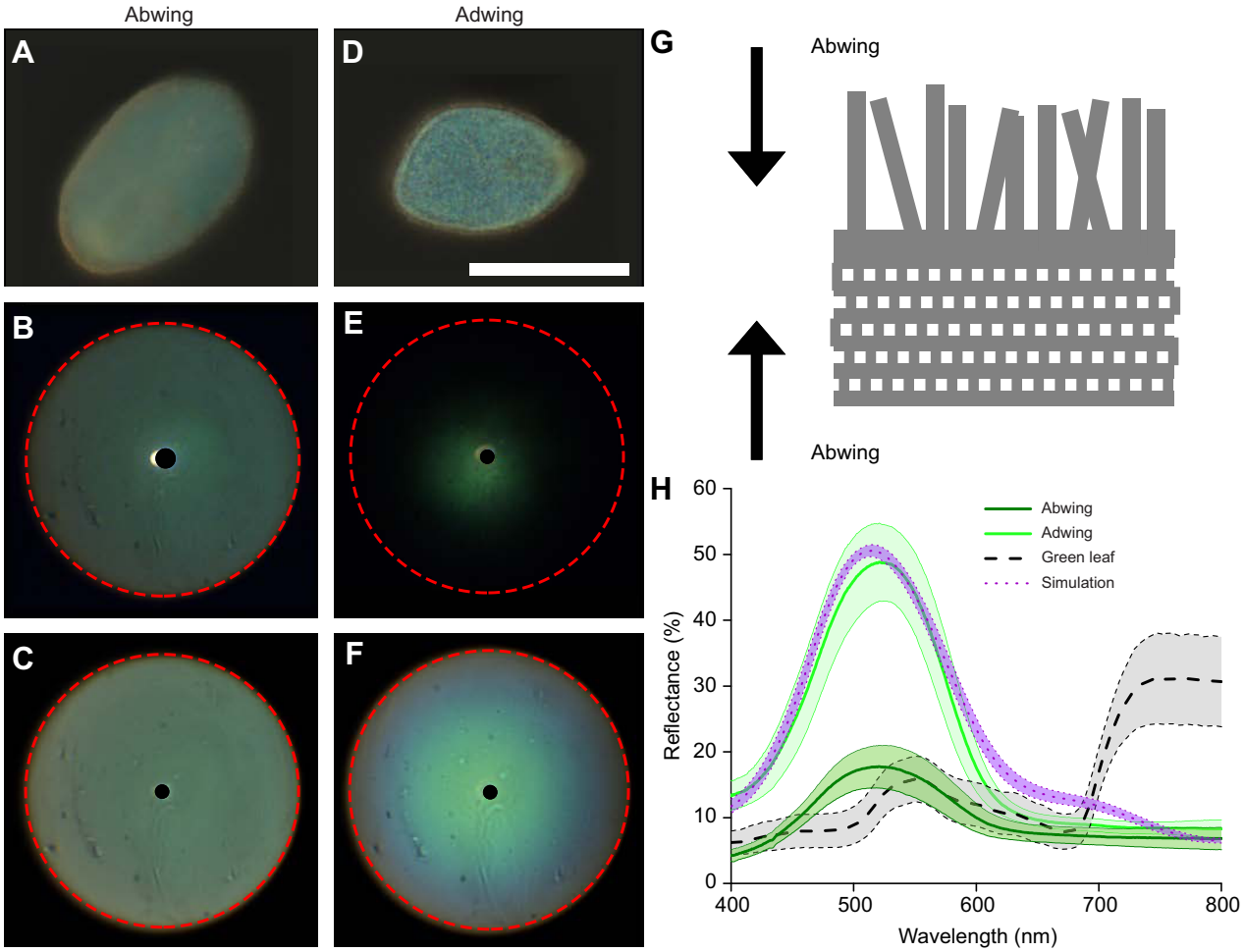

Fig. 3. *k*-space imaging and reflectance spectra of *H. argentea* scales. (A–C) Upper, abwing side; (D–F) lower, adwing side. *k*-space imaging was performed under narrow- (B,E) and wide-aperture (C,F) illumination. The red dashed circle represents the aperture of the objective, corresponding to a scattering angle of ∼71 deg. Scale bar: 50 µm. (G) Schematic representation of a scale. Dark arrows represent the direction of the incoming light for abwing and adwing measurements. (H) The reflection of the different sides compared with that of a green leaf. Solid lines represent experimental measurement of abwing and adwing scales (*N*=9 and 8, respectively). The dashed line is the reflection of a green leaf (*N*=10). The dotted purple line is a simulated reflectance spectrum of a multilayer photonic crystal without diffusive elements. All curves show means±s.d.

from the abwing side (Fig. 3A), the reflected light was uniformly scattered to all angles (Fig. 3B), indicating a diffuse reflection. When illuminated from the adwing side, the reflection was highly specular (Fig. 3D,E), indicating that the adwing side of the scale is reflecting the light in a manner similar to a mirror. Under wide-aperture illumination, the light reflected from the abwing (Fig. 3A) was chromatically uniform at all angles (Fig. 3C), while the reflection from the adwing side showed that the reflection varied from green at normal incidence to blue at high incidence angles, typical of iridescence due to a multilayered structure (Fig. 3F).

The reflectance of a single scale was spectrally characterized using a spectrometer coupled to a microscope, using epi-illumination from the abwing (filament) and adwing (multilayer) sides (Fig. 3G). While the spectral shape was similar, the peak reflectance was ∼20% and ∼50% for the abwing and adwing side, respectively (Fig. 3H). For comparison, a typical reflection from a green leaf peaks at around 550 nm, with peak reflectance of ∼15%, comparable to the abwing reflection. We modelled the reflectance using a common multilayer model (Stavenga et al., 2011a) with the material parameters obtained from ultrastructure. The modelled spectrum (dotted line in Fig. 3H) approximated well the measured reflectance of the adwing side.

DISCUSSION

Diffusive reflection in *H. argentea*

The dull green colour of *H. argentea* results from a combination of a multilayer structure, an absorbing pigment and a filamentous diffuser. The ultrastructure of the scale is composed of two parts where a disordered brush-like layer overlies a periodic multilayer structure. This brush-like layer diffuses the light incident onto and reflected by the multilayer structure into the whole hemisphere. This eliminates the iridescence that is native to a periodic multilayer structure, thereby supressing the blue-shift at non-normal incidence or reflection angles, as seen in the adwing scatterogram in Fig. 3F. This results in a spectral and spatial reflectance pattern of the beetle elytra that is similar to that of plant leaves (Fig. 3H).

The addition of the filamentous layer to the beetle scale has a dramatic effect on the appearance of *H. argentea* when compared with the brilliant blue-coloured *H. coerulea* (Gentil, 1943; Vigneron et al., 2005). It is noteworthy that the fluorescent pigmentation (see Fig. 2B,D; Fig. S2; see also Mouchet et al., 2016c, 2019) and the photonic structures are very similar in the two beetles, with a slightly increased layer-to-layer distance in *H. argentea* (195 nm) compared with *H. coerulea* (175 nm) (Mouchet et al., 2016b; Rassart et al., 2009), resulting in reflection peaks in the green and

blue, respectively. This suggests that the fabrication of the photonic structure is evolutionarily adaptable. We have not explored the change of colour due to wetting in *H. argentea*, but it is probably also present given it has a similar porous structure to *H. coerulea*. In the future, it may be worthwhile to explore whether wetting might cause the apparent diversity of the dorsal coloration (between green and yellow), and whether the colour change has any influence on intraspecific recognition (Briscoe and Chittka, 2001).

Camouflage by spectral filtering

The intensity and the uniform scattering of light reflected from *H. argentea* scales resemble the chlorophyll-based pigment reflection of green leaves in the part of the spectrum relevant for vision (320–650 nm; see Figs 1A and 3H). To mimic plant reflection, *H. argentea* combines a spectrally selective, directional reflector with a pigment absorber and a diffuser in the scale ultrastructure. This suggests a function in camouflage, a commonly used survival strategy where animals try to reduce their visibility by mimicking the coloration of their environment. *Hoplia argentea* is not the first insect found to be using a photonic strategy to hide in a foliaceous background. Many insects have employed similar strategies to decrease the iridescence of a photonic structure and to achieve a reflectance very close to that of chlorophyll-based plants. For example, some butterflies combine a gyroid photonic crystal with pigmentary attenuation and spatial filtering (Wilts et al., 2012b, 2017). Between their lower and upper lamina, the wing scales of *Parides* butterflies have a gyroid nanostructure acting as a selective reflector for green colour (Wilts et al., 2017). The reflected green light is filtered when it passes through a thick upper lamina that contains pigments. Quite similar to the beetle scales described here, this stacking results in spatial distribution of the reflection that is almost angle independent. A combination of pigments and structural reflection is also present in the green feathers of some parrots (Stavenga et al., 2011b) and budgerigars (D'Alba et al., 2012). Stable coloration by complex photonic morphologies has also been observed in dragonflies (Nixon et al., 2015), where a wrinkled multilayer spreads the reflected signal over a large angular range.

Other strategies are based on the nanostructures alone, where the dimensions of the ordered nanostructure play an important role. As an example, the long-range order of diamond photonic crystals has been investigated in weevils (Nagi et al., 2018; Wilts et al., 2013a). In contrast to the highly specular reflection arising from a long-range ordered structure in *Entimus imperialis*, *Eupholus cuvieri* possesses multiple structural domains within the same scale. Those domains have different orientations, resulting in colour mixing and a rather diffuse green reflection (Wilts et al., 2013a), which facilitates camouflage.

Biological significance of the coloration

In *H. coerulea*, the ventral sides of both sexes are covered with bright scales, while the dorsal sides are strongly dimorphic: the males have specular blue elytra, while the females are dull brown (Rassart et al., 2009). In contrast, *H. argentea* investigated here does not show a sexual dimorphism as both sexes have a dull green to orange dorsal colour, while the ventral colour is blue–green iridescent. Dimorphism in monkey beetles is thought to be associated with day-active, flower-visiting taxa where the coloration is supposed to serve in display and mimicry (Ahrens et al., 2011). Our results add camouflage as yet another possible function. To that end, it is interesting that two related species found in Europe, *H. coerulea* and *H. argentea*, with seemingly similar ecology in terms of dwelling on flowers, have evolved diverse coloration strategies and strong differences in dimorphism.

Further, we were surprised by the observation that the ventral blue–green colour (Fig. S3) seems to be more consistent over the life time of a beetle than the dorsal colour, as the ventral scales seem to shed less than the dorsal scales (Fig. S4). The colour of the dorsal side therefore seems to be somewhat variable (with small shifts in the peak wavelength) in this species and we can list three possible contributing factors leading to this: (i) the scales may have slightly different structural properties among individuals (similar to differences between *H. coerulea* and *H. argentea*); (ii) the colour is influenced by humidity-dependent wetting, and (iii) the overall hue changes from green towards brown as a result of shedding of scales from the elytra. Pending further studies, we hypothesize that this colour change may actually be beneficial to the survival of females as they progress from dwelling on plants, where they feed and mate, to laying eggs on the soil.

Conclusion

Here, we characterized the coloration mechanism in the green-coloured scales of *H. argentea*. To achieve an angle-independent green reflection, the scale ultrastructure combines a multilayer photonic crystal below with a disordered layer of hair-like filaments. The reflected colour is mainly determined by the photonic crystal and then scattered by passing through the filament layer. This results in light reflection with a homogeneous angular distribution, mimicking common leaf coloration, and thereby providing an efficient camouflage strategy. Further, the species of the genus *Hoplia* seem to be employing different coloration strategies, and these differences may be related to their different life styles.

Acknowledgements

We thank Felipe Saenz for his help with the fluorimetry experiment, Gregor Belušič for supplying some of the animals and Al Vrezec for discussions on the species biology and for supplying the taxonomic literature. We are grateful to Pierre-Paul Bitton and the other anonymous reviewer(s) for useful comments on the manuscript.

Competing interests

The authors declare no competing or financial interests.

Author contributions

Conceptualization: C.K., B.W.; Methodology: C.K., P.P., B.W.; Formal analysis: C.K., B.W.; Investigation: C.K., P.P., B.W.; Data curation: C.K.; Writing - original draft: C.K., P.P., U.S., B.W.; Visualization: C.K., P.P.; Supervision: B.W.; Funding acquisition: U.S., B.W.

Funding

This study was supported by the Swiss National Science Foundation (Schweizerischer Nationalfonds zur Förderung der wissenschaftlichen Forschung) through project grant 163220 (to U.S.), Ambizione programme grant 168223 (to B.D.W.), and the National Centre of Competence in Research Bio-inspired Materials. This study was supported by the infrastructural centre for Microscopy of Biological Samples at Biotechnical Faculty, University of Ljubljana.

Supplementary information

Supplementary information available online at
http://jeb.biologists.org/lookup/doi/10.1242/jeb.213306.supplemental

References

Ahrens, D., Scott, M. and Vogler, A. P. (2011). The phylogeny of monkey beetles based on mitochondrial and ribosomal RNA genes (Coleoptera: Scarabaeidae: Hopliini). *Mol. Phylogenet. Evol.* **60**, 408-415. doi:10.1016/j.ympev.2011.04.011

Berthier, S. (2007). *Iridescences*. New York, NY: Springer.

Biró, L. P. and Vigneron, J. P. (2011). Photonic nanoarchitectures in butterflies and beetles: valuable sources for bioinspiration. *Laser Photon. Rev.* **5**, 27-51. doi:10.1002/lpor.200900018

Bradbury, J. W. and Vehrencamp, S. L. (2011). *Principles of Animal Communication*. Oxford: Oxford University Press.

Brelih, S., Kajzer, A. and Pirnat, A. (2010). Material for the beetle fauna (Coleoptera) of Slovenia 4th contribution: Polyphaga: Scarabaeoidea (=Lamellicornia). *Scopolia* **70**, 1-386.
Briscoe, A. D. and Chittka, L. (2001). The evolution of color vision in insects. *Annu. Rev. Entomol.* **46**, 471-510. doi:10.1146/annurev.ento.46.1.471
D'Alba, L., Kieffer, L. and Shawkey, M. D. (2012). Relative contributions of pigments and biophotonic nanostructures to natural color production: a case study in budgerigar (*Melopsittacus undulatus*) feathers. *J. Exp. Biol.* **215**, 1272-1277. doi:10.1242/jeb.064907
Doucet, S. M. and Meadows, M. G. (2009). Iridescence: a functional perspective. *J. R. Soc. Interface* **6**, S115-S132. doi:10.1098/rsif.2008.0395.focus
Gentil, K. (1943). Beitrag zur Morphologie und Optik der Schillerschuppen von *Hoplia coerulea* Drury und *Hoplia farinosa* Linné (col.). *Z. Morphol. Ökolog. Tiere* **40**, 299-313. doi:10.1007/BF00421686
Holt, A. L., Sweeney, A. M., Johnsen, S. and Morse, D. E. (2011). A highly distributed Bragg stack with unique geometry provides effective camouflage for Loliginid squid eyes. *J. R. Soc. Interface* **8**, 1386-1399. doi:10.1098/rsif.2010.0702
Hubbs, C. L. (1942). Adaptive coloration of animals. *Am. Nat.* **76**, 500. doi:10.1086/281046
Johnsen, S. (2001). Hidden in plain sight: the ecology and physiology of organismal transparency. *Biol. Bull.* **201**, 301-318. doi:10.2307/1543609
Jordan, T. M., Partridge, J. C. and Roberts, N. W. (2012). Non-polarizing broadband multilayer reflectors in fish. *Nat. Photonics* **6**, 759-763. doi:10.1038/nphoton.2012.260
Mouchet, S. R., Van Hooijdonk, E., Welch, V. L., Louette, P., Colomer, J.-F., Su, B.-L. and Deparis, O. (2016a). Liquid-induced colour change in a beetle: the concept of a photonic cell. *Sci. Rep.* **6**, 19322. doi:10.1038/srep19322
Mouchet, S. R., Tabarrant, T., Lucas, S., Su, B.-L., Vukusic, P. and Deparis, O. (2016b). Vapor sensing with a natural photonic cell. *Opt. Express* **24**, 12267. doi:10.1364/OE.24.012267
Mouchet, S. R., Lobet, M., Kolaric, B., Kaczmarek, A. M., Van Deun, R., Vukusic, P., Deparis, O. and Van Hooijdonk, E. (2016c). Controlled fluorescence in a beetle's photonic structure and its sensitivity to environmentally induced changes. *Proc. R. Soc. B Biol. Sci.* **283**, 20162334. doi:10.1098/rspb.2016.2334
Mouchet, S. R., Lobet, M., Kolaric, B., Kaczmarek, A. M., Van Deun, R., Vukusic, P., Deparis, O. and Van Hooijdonk, E. (2017). Photonic scales of *Hoplia coerulea* beetle: any colour you like. *Materials Today: Proc.* **4**, 4979-4986. doi:10.1016/j.matpr.2017.04.104
Mouchet, S. R., Verstraete, C., Mara, D., Van Cleuvenbergen, S., Finlayson, E. D., Van Deun, R., Deparis, O., Verbiest, T., Maes, B., Vukusic, P. et al. (2019). Nonlinear optical spectroscopy and two-photon excited fluorescence spectroscopy reveal the excited states of fluorophores embedded in a beetle's elytra. *Interface Focus* **9**, 20180052. doi:10.1098/rsfs.2018.0052
Nagi, R. K., Montanari, D. E. and Bartl, M. H. (2018). Photonic crystal micro-pixelation and additive color mixing in weevil scales. *Bioinspir. Biomim.* **13**, 035003. doi:10.1088/1748-3190/aaaf55
Nixon, M. R., Orr, A. G. and Vukusic, P. (2015). Wrinkles enhance the diffuse reflection from the dragonfly *Rhyothemis resplendens*. *J. R. Soc. Interface* **12**, 20140749. doi:10.1098/rsif.2014.0749
Rassart, M., Simonis, P., Bay, A., Deparis, O. and Vigneron, J. P. (2009). Scale coloration change following water absorption in the beetle *Hoplia coerulea* (Coleoptera). *Phys. Rev. E Stat. Nonlinear Soft Matter Phys.* **80**, 031910. doi:10.1103/PhysRevE.80.031910
Schaefer, H. M. and Stobbe, N. (2006). Disruptive coloration provides camouflage independent of background matching. *Proc. R. Soc. B Biol. Sci.* **273**, 2427-2432. doi:10.1098/rspb.2006.3615
Seago, A. E., Brady, P., Vigneron, J.-P. and Schultz, T. D. (2009). Gold bugs and beyond: a review of iridescence and structural colour mechanisms in beetles (Coleoptera). *J. R. Soc. Interface* **6**, S165-S184. doi:10.1098/rsif.2008.0354.focus
Siddique, R. H., Gomard, G. and Hölscher, H. (2015). The role of random nanostructures for the omnidirectional anti-reflection properties of the glasswing butterfly. *Nat. Commun.* **6**, 6909. doi:10.1038/ncomms7909
Srinivasarao, M. (1999). Nano-optics in the biological world: beetles, butterflies, birds, and moths. *Chem. Rev.* **99**, 1935-1962. doi:10.1021/cr970080y
Stavenga, D. G., Wilts, B. D., Leertouwer, H. L. and Hariyama, T. (2011a). Polarized iridescence of the multilayered elytra of the Japanese jewel beetle, *Chrysochroa fulgidissima*. *Philos. Trans. R. Soc. B Biol. Sci.* **366**, 709-723. doi:10.1098/rstb.2010.0197
Stavenga, D. G., Tinbergen, J., Leertouwer, H. L. and Wilts, B. D. (2011b). Kingfisher feathers - colouration by pigments, spongy nanostructures and thin films. *J. Exp. Biol.* **214**, 3960-3967. doi:10.1242/jeb.062620
Stavenga, D. G., Leertouwer, H. L. and Wilts, B. D. (2013). Quantifying the refractive index dispersion of a pigmented biological tissue using Jamin-Lebedeff interference microscopy. *Light Sci. Appl.* **2**, e100. doi:10.1038/lsa.2013.56
Stevens, M. and Merilaita, S. (2011). *Animal Camouflage* (ed. M. Stevens and S. Merilaita), Cambridge: Cambridge University Press.
Vigneron, J. P., Colomer, J.-F., Vigneron, N. and Lousse, V. (2005). Natural layer-by-layer photonic structure in the squamae of *Hoplia coerulea* (Coleoptera). *Phys. Rev. E Stat. Nonlinear Soft Matter Phys.* **72**, 061904. doi:10.1103/PhysRevE.72.061904
Vukusic, P., Kelly, R. and Hooper, I. (2009). A biological sub-micron thickness optical broadband reflector characterized using both light and microwaves. *J. R. Soc. Interface* **6**, S193-S201. doi:10.1098/rsif.2008.0345.focus
Wilts, B. D., Trzeciak, T. M., Vukusic, P. and Stavenga, D. G. (2012a). Papiliochrome II pigment reduces the angle dependency of structural wing colouration in *nireus* group papilionids. *J. Exp. Biol.* **215**, 796-805. doi:10.1242/jeb.060103
Wilts, B. D., Michielsen, K., De Raedt, H. and Stavenga, D. G. (2012b). Iridescence and spectral filtering of the gyroid-type photonic crystals in *Parides sesostris* wing scales. *Interface Focus* **2**, 681-687. doi:10.1098/rsfs.2011.0082
Wilts, B. D., Ijbema, N., Michielsen, K., De Raedt, H. and Stavenga, D. G. (2013a). Shine and hide: biological photonic crystals on the wings of weevils. *Materials Research Society Symposium Proceedings*, pp. 1-6. doi:10.1557/opl.2013.184
Wilts, B. D., Pirih, P., Arikawa, K. and Stavenga, D. G. (2013b). Shiny wing scales cause spec(tac)ular camouflage of the angled sunbeam butterfly, *Curetis acuta*. *Biol. J. Linn. Soc.* **109**, 279-289. doi:10.1111/bij.12070
Wilts, B. D., Apeleo Zubiri, B., Klatt, M. A., Butz, B., Fischer, M. G., Kelly, S. T., Spiecker, E., Steiner, U. and Schröder-Turk, G. E. (2017). Butterfly gyroid nanostructures as a time-frozen glimpse of intracellular membrane development. *Sci. Adv.* **3**, e1603119. doi:10.1126/sciadv.1603119
Yeh, P. (2005). *Optical Waves in Layered Media*. Hoboken, NJ: Wiley.
Yoshida, A., Motoyama, M., Kosaku, A. and Miyamoto, K. (1996). Nanoprotuberance array in the transparent wing of a hawkmoth, *Cephonodes hylas*. *Zoolog. Sci.* **13**, 525-526. doi:10.2108/zsj.13.525